Volume 4 | Number 20 | 28 May 2016 | Pages 3411–3622

Journal of Materials Chemistry B

Materials for biology and medicine

www.rsc.org/MaterialsB

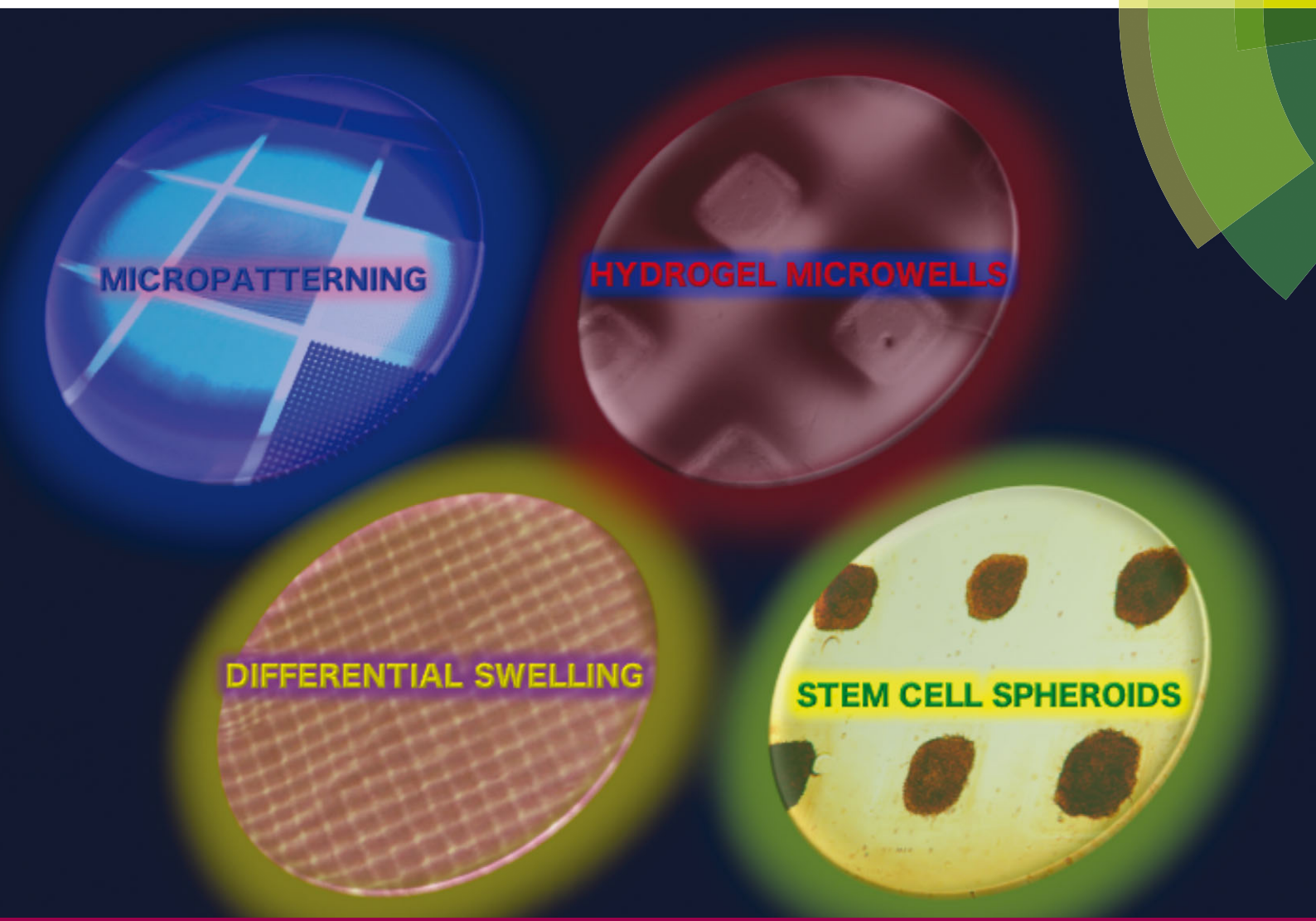

Themed issue: Stem Cells

ISSN 2050-750X

ROYAL SOCIETY OF CHEMISTRY

PAPER

Eben Alsberg *et al.*

Dual-crosslinked hydrogel microwell system for formation and culture of multicellular human adipose tissue-derived stem cell spheroids

175 YEARS

Journal of Materials Chemistry B

PAPER

Cite this: J. Mater. Chem. B, 2016, 4, 3526

Dual-crosslinked hydrogel microwell system for formation and culture of multicellular human adipose tissue-derived stem cell spheroids

Oju Jeon,[a] Robyn Marks,[a] David Wolfson[a] and Eben Alsberg*[ab]

Received 9th January 2016,
Accepted 5th April 2016

DOI: 10.1039/c6tb00064a

www.rsc.org/MaterialsB

Three-dimensional (3D) multicellular spheroids of human adipose tissue-derived stem cells (hASCs) are an attractive system for basic science studies and tissue engineering applications, as they can resemble cellular condensations present in developmental and healing processes. The purpose of this study was to engineer a hydrogel-based microwell platform by capitalizing on the differential swelling behavior of micropatterned dual-crosslinked oxidized, methacrylated alginate (OMA)/multi-arm polyethylene glycol (PEG) hydrogels for rapid formation of uniform multicellular hASC spheroids with controllable size and evaluation of the capacity of the system to be used to drive osteogenic differentiation of the spheroids. By changing the micropattern size, the size of the hydrogel microwells was easily controllable. Microwell-seeded hASCs generated spheroids of relatively uniform size and high cell viability. hASC spheroids exhibited rapid mineralization in osteogenic media, which was faster than that of conventional two-dimensionally cultured hASCs. This new hydrogel microwell system has great potential for controlled multicellular spheroid formation and defined signal presentation from the hydrogel material to the cell aggregates to regulate tissue formation.

Introduction

Stem cells represent an attractive cell source for tissue engineering applications due to their high proliferative capacity and multilineage differentiation potential when treated with established conditions.[1,2] Mesenchymal stem cells, which are easily obtained from bone marrow, adipose tissue, umbilical cord blood, muscle, bone and cartilage, are employed extensively in strategies attempting to regenerate lost or damaged tissues.[3–6] In particular, human adipose-derived stem cells (hASCs) can be isolated from fat tissue in significant numbers,[5,7] exhibit stable growth in two-dimensional (2D) culture and, when provided with specific signals, can differentiate down the osteogenic,[8] adipogenic[9] and chondrogenic[10] lineages. However, traditional 2D systems fail to provide a physiological cell microenvironment, where cells are surrounded by other cells and extracellular matrix, often resulting in loss of desired differentiated cell phenotypes.[11–13]

In contrast, growing stem cells in three-dimensional (3D) multicellular spheroids,[14–17] which can resemble cellular condensations present in native tissue development and healing,[18,19] is a potentially valuable approach for recreating these physiologically relevant microenvironments to guide new tissue formation for regenerative medicine applications. Microwell systems have been widely used to generate multicellular spheroids such as embryonic bodies,[20] neurospheres,[21] pancreatic beta-cell aggregates[22] or cancer spheroids.[23] While the classical hanging drop method[24,25] provides some control over the spheroid size but is a labor-intensive technique, a microwell system not only provides a facile strategy to enhance the throughput but also yields more homogeneous, size- and shape-controlled cell aggregates.[20,26] However, commercial microwell systems do not currently permit user modulation of spheroid size. To our knowledge, there are currently no microwell systems with the capacity for spatial or temporal control over the presentation of physical and biochemical signals from the culture substrate itself.

The purpose of this study was to develop biocompatible and biodegradable hydrogel-based microwells by capitalizing on the differential swelling behavior of micropatterned dual-crosslinked hydrogels[2,27] comprised of both oxidized methacrylated alginate (OMA)[28] and 8-arm poly(ethylene glycol) amine (PEG).[29] This system was utilized to rapidly form multicellular hASC spheroids with controllable size and evaluated to determine its capacity to drive osteogenic differentiation of the spheroids by delivering bone morphogenetic protein-2 (BMP-2) from the OMA/PEG hydrogel microwells. This micropatterned dual-crosslinked OMA/PEG hydrogel microwell system may provide

[a] Department of Biomedical Engineering, Case Western Reserve University, Cleveland, OH 44106, USA. E-mail: eben.alsberg@case.edu
[b] Department of Orthopaedic Surgery, Case Western Reserve University, Cleveland, OH 44106, USA

a useful platform for studying the role of spatiotemporally controlled biomaterial physical and biochemical properties on cell spheroid behavior.

Materials and methods

Microfabrication of micropatterned, dual-crosslinked hydrogel microwells

The OMA macromer (20% actual oxidation and 22% actual methacrylation) was prepared as previously described.[2,28] Eight-arm poly(ethylene glycol)-amine hydrochloric acid salt (8-arm PEG amine·HCl, 20 g, M_w = 10 000 Da, Jenkem Technology USA Inc., Allen, TX) was dissolved in 100 ml of methylene chloride (Fisher Scientific, Pittsburgh, PA), and triethylamine (the mole ratio of triethylamine to HCl of 8-arm PEG amine·HCl = 2, Fisher Scientific) was added into the PEG solution to remove HCl salt from the 8-arm PEG amine HCl. After 24 h, the solution was precipitated into excess of hexanes (Fisher Scientific), dried under reduced pressure and rehydrated to a 10% w/v solution in ultrapure deionized water (diH_2O) for further purification. The 8-arm PEG amine was further purified by dialysis against diH_2O (MWCO 3500; Spectrum Laboratories Inc., Rancho Dominguez, CA) for 3 days, filtered (0.22 μm filter, Fisher Scientific) and lyophilized. OMA (20% w/v) and 8-arm PEG amines (40% w/v) were separately dissolved in Dulbecco's Modified Eagle Medium (DMEM, Sigma, St. Louis, MO) with 0.05% w/v photoinitiator [2-hydroxy-4′-(2-hydroxyethoxy)-2-methylpropiophenone, Sigma]. To create the single-crosslinked hydrogel by Schiff base reaction between the aldehyde groups of the OMA and the amine groups of the 8-arm PEG, 300 μl of OMA solution was mixed with the 8-arm PEG amine solution at an equal volume ratio for 1 min. Immediately after mixing the two solutions, the resultant mixture was injected between quartz (top) and glass (bottom) plates separated by 0.75 mm spacers, and incubated for 30 min. Subsequently, a photomask with grid patterns was placed on top of the quartz plate, and a micropatterned dual-crosslinked hydrogel was formed by exposure to UV light (320–500 nm, EXFO OmniCure S1000-1B, Lumen Dynamics Group, Mississauga, Ontario, Canada) at 3.5 mW cm^{-2} through the photomask for 1 min. Differential swelling of the micropatterned dual-crosslinked hydrogels was induced in diH_2O, DMEM or Dulbecco's phosphate-buffered saline (DPBS) containing 0.05% w/v photoinitiator for 10 min, and then the resulting hydrogel microwells that were formed were stabilized by applying UV light again for 1 min. The wall heights of the hydrogel microwells (as shown in cross section in Fig. 2(c)) were measured using a microscope (ECLIPSE TE 300, Nikon, Tokyo, Japan). Photomasks with different grid pattern dimensions (100 and 500 μm) were used to generate hydrogel microwells with different well sizes. Fluorescent hydrogels were prepared with methacryloxyethyl thiocarbamoyl rhodamine B (0.01% w/v, Polysciences Inc., Warrington, PA) mixed into the macromer solution. The unreacted fluorophore from the single-crosslinked regions was removed by extracting and washing the hydrogels with DPBS for 30 min. Hydrogel microwells were imaged using a fluorescence microscope (ECLIPSE TE 300) equipped with a digital camera (Retiga-SRV, Qimaging, Burnaby, BC, Canada).

To immobilize heparin onto the bottom of hydrogel microwells, methacrylated heparin (MH)[30] (0.1% w/v) was mixed separately into the OMA solution and the 8-arm PEG macromer solution, 300 μl of OMA/MH solution was mixed with the 8-arm PEG amine/MH solution at an equal volume ratio for 1 min. The resultant mixture was then immediately injected between quartz (top) and glass (bottom) plates separated by 0.4 mm spacers, and incubated for 30 min. A photomask with a 500 μm grid pattern was placed on top of the quartz plate to form a micropatterned dual-crosslinked hydrogel as described earlier. The unreacted MH from the single-crosslinked regions was removed by washing the hydrogels in DPBS containing 0.05% w/v photoinitiator for 20 min, and then the hydrogel microwells were stabilized as described earlier. Toluidine blue O staining of hydrogels was performed as previously reported.[31,32] Stained heparin in the hydrogel microwells was visualized using a microscope (Leitz Laborlux S, Leica, Germany) equipped with a digital camera (Coolpix 995, Nikon, Japan).

To evaluate the shear storage modulus of dual-crosslinked OMA/PEG hydrogels, the OMA macromers with various degrees of oxidation were prepared as previously reported.[2,28] The actual degrees of oxidation and methacrylation were calculated from ^{1}H-NMR spectra as previously reported.[27,28] The actual degrees of alginate oxidation were 9%, 14%, and 20%. The actual degrees of methacrylation of each OMA were 19%, 21% and 25%, respectively. To fabricate dual-crosslinked OMA/PEG hydrogels, the OMA/PEG mixtures were injected between two glass plates separated by 0.75 mm spacers, incubated for 30 min to form single-crosslinked hydrogels, and then photo-crosslinked with 365 nm UV light (Model EN-280L, Spectroline, Westbury, NY) placed on top of the upper plate at ~1 mW cm^{-2} for 15 min to form the dual-crosslinked hydrogels. Dual-crosslinked OMA/PEG hydrogel disks were created using an 8 mm diameter biopsy punch and placed in an incubator at 37 °C for 30 min. The shear storage modulus of the dual-crosslinked hydrogels was measured using a strain-controlled AR-2000ex rheometer (TA Instruments, New Castle, DE) with stainless-steel parallel plate geometry (plate diameter of 8 mm, gap of 0.7–0.8 mm) at 25 °C. The measurements were performed using a dynamic frequency sweep test in which a sinusoidal shear strain of constant peak amplitude (0.2%) was applied over a range of frequencies (0.6–100 rad s^{-1}). Since the hydrogels exhibited a plateau of the storage modulus over the frequency range examined, the shear storage modulus at 10 rad s^{-1} of the dual-crosslinked OMA/PEG hydrogels was reported (N = 3).

Formation of multicellular 3D hASC spheroids

hASCs were isolated from the adipose tissue using a previously reported method.[33] Briefly, lipoaspirates were digested with 200 unit per mg collagenase type I (Worthington Biochemical Products, Lakewood, NJ) for 40 min at 37 °C. The stromal fraction was then isolated by density centrifugation and the stromal cells were plated at 3500 cell per cm^2 on tissue

culture plastic in DMEM/nutrient mixture F12 (DMEM/F12, BioWhittaker, Suwance, GA) with 10% defined fetal bovine serum (FBS, HyClone, Logan, UT), 100 U ml^{-1} penicillin and 100 μg ml^{-1} streptomycin (1% P/S, BioWhittaker). hASCs at passage 3 were seeded on the hydrogel microwells (5×10^4 cells per cm^2) in 96-well plates and centrifuged at 300 × *g* for 5 min to force cell accumulation into the microwells. To evaluate the homogeneity of multicellular spheroid populations, the diameters of multicellular spheroids were measured using NIH Image J analysis software after 1 day of culture ($N = 24$ per group). hASC spheroids in the hydrogel microwells were maintained in 96-well plates with 100 μl DMEM/F12 containing 10% FBS and 1% P/S with media changes two times a week. At predetermined time points, the viability and morphology of the resulting multicellular hASC spheroids in the hydrogel microwells were examined using a Live/Dead assay comprised of fluorescein diacetate (FDA, Sigma) and ethidium bromide (EB, Sigma). 2 μl of staining solution was added into each well and incubated for 3–5 min at room temperature, and then stained multicellular hASC spheroids were imaged using the fluorescence microscope and digital camera.

Osteogenic differentiation of multicellular 3D hASC spheroids

To form hASC spheroids in BMP-2 (Department of Developmental Biology, University of Würzburg, Germany) laden dual-crosslinked OMA/PEG hydrogel microwells, 2 μg BMP-2 was added to 500 μl of each macromer solution, and then micropatterned dual-crosslinked hydrogels were formed as described above. Hydrogel disks were created using a 3 cm diameter biopsy punch. Differential swelling of the micropatterned dual-crosslinked hydrogels was induced in 1 ml diH_2O containing 0.05% w/v photoinitiator for 10 min in 6-well tissue culture plate, and then the resulting hydrogel microwells that were formed were stabilized by applying UV light (3.5 mW cm^{-2}) again for 1 min and further incubated in 1 ml DMEM/F12 with 10% FBS. To form multicellular hASC spheroids, hASCs (5×10^5 cells) at passage 3 were seeded on the hydrogel microwells in 6-well plates and centrifuged at 300 × *g* for 5 min to force cell aggregation into the wells. After 1 day of culture, hydrogel microwells containing multicellular hASC spheroids were transferred to 100 ml spinner flasks (Bellco Glass Inc., Vineland, NJ) containing 54 ml DMEM/F12 with 10% defined FBS and 1% P/S (Microwell group, 10 hydrogel microwells per flask, $N = 3$ flasks). The spinner flasks were placed in a humidified incubator at 37 °C with 5% CO_2 and stirred at 40 rpm. After 2 days of culture, the media was replaced with osteogenic media [10 mM β-glycerophosphate (CalBiochem, Billerica, MA), 50 μM ascorbic acid (Wako USA, Richmond, VA), and 100 nM dexamethasone (MP Biomedicals, Solon, OH) in DMEM-high glucose] containing 10% FBS and 1% P/S. The osteogenic media was changed twice a week. As a comparative group (Suspension group), suspended hASCs (5.4×10^6 cells) were cultured in spinner flasks containing 54 ml DMEM/F12 with 10% FBS and 1% P/S, and the media was replaced with osteogenic media containing 100 ng ml^{-1} BMP-2 after 2 days of culture ($N = 3$ flasks). The osteogenic media containing 100 ng ml^{-1} BMP-2 was changed two times a week. The osteogenic differentiation of hASCs in osteogenic media containing 100 ng ml^{-1} BMP-2 in two-dimensions on tissue culture plastic served as a positive control group (2D group). At predetermined time points, 10 ml of conventional suspension (Suspension) and microwell (Microwell) cultured multicellular hASC spheroids were removed from each spinner flask, fixed in 4% paraformaldehyde for 40 min after aspirating media, washed three times with DPBS, and stained with 2% Alizarin red S solution (pH 4.2) at room temperature for 5 min. After washing for 30 min with diH_2O three times, the stained multicellular hASC spheroids were imaged using a microscope (Leitz Laborlux S, Leica, Germany) equipped with a digital camera (Coolpix 995, Nikon, Japan). The 2D cultured hASCs serving as a positive control were similarly stained with Alizarin red S and imaged. To quantify the calcium content, additional 10 ml multicellular hASC spheroid suspensions were taken from the spinner flasks. After aspirating media, the multicellular hASC spheroids were homogenized on ice in 1 ml cell lysis buffer (Sigma) at 35 000 rpm for 60 s using a TH homogenizer (Omni International, Marietta, GA). After centrifuging at 16 200 × *g* for 10 min, 100 μl of supernatant was mixed with 100 μl of 1 × Tris-EDTA buffer (Invitrogen, Carlsbad, CA) containing fluorescent PicoGreen® reagent (Invitrogen) and incubated at room temperature for 30 min. Fluorescence intensity of the dye-conjugated DNA solution was measured in 96-well plates on a plate reader (480 nm excitation and 520 nm emission, SAFIRE, Tecan, Austria), and the DNA content was calculated from a standard curve generated with calf thymus DNA (Invitrogen). Calcium content of the multicellular hASC spheroids was quantified using a calcium assay kit (Pointe Scientific, Canton, MI) according to the company's instructions. The supernatant (4 μl) was mixed with a color and buffer reagent mixture (250 μl), and the absorbance was read at 570 nm on the plate reader. To evaluate the homogeneity of multicellular spheroid populations, the diameters of multicellular spheroids were measured using NIH ImageJ analysis software ($N > 100$ per group).

Statistical analysis

All quantitative data is expressed as mean ± standard deviation. Statistical analysis was performed with one-way analysis of variance (ANOVA) with Tukey significant difference *post hoc* test using Origin software (OriginLab Co., Northampton, MA). A value of $p < 0.05$ was considered statistically significant.

Results and discussion

Fabrication of dual-crosslinked OMA/PEG hydrogel microwells

Since the differentiation of stem cells has been enhanced by 3D spheroid culture,[34–36] the use of multicellular spheroids is an attractive option for tissue engineering.[14,33,37] Conventional approaches of fabricating multicellular spheroids, such as hanging drop and spinner flask culture, typically suffer from low throughput and/or polydispersity in spheroid size.[38,39] To overcome these limitations, microwell techniques have been developed for rapid and high-throughput production of

multicellular spheroids with narrow size distribution.[22,40–43] However, the traditional microwell techniques provide limited capacity to present defined cues from the microwells themselves (*e.g.*, controlled deliver of bioactive factors and varying microwell mechanical and cell adhesive properties) for regulating cell behavior in the spheroids.[37,44] In this study, 3D dual-crosslinked micropatterned hydrogel microwells have been engineered to provide a simple and reproducible way to produce large numbers of spheroids while modulating their size and delivering BMP-2 from the microwells using micropatterned dual-crosslinkable OMA/PEG hydrogels. It is anticipated that this hydrogel system may also be modified to spatiotemporally control the presentation of other physical and/or biochemical signals, such as its stiffness or cell adhesivity, from the hydrogel microwells themselves to regulate stem cell fate.[2,6,45]

The overall strategy for the formation of the dual-crosslinked OMA/PEG hydrogel microwells is depicted in Fig. 1(a). The first crosslinked networks were formed by Schiff base reaction between the amine groups of the 8-arm PEG and the aldehyde groups of the OMA (Fig. 1(b)). The second crosslinked networks were formed by photocrosslinking the methacrylate groups of the OMA in the single-crosslinked OMA/PEG hydrogels thorough photomasks with a grid pattern (Fig. 1(b)). The grid micropattern was visually confirmed using photocrosslinkable methacrylated rhodamine B (Fig. 1(b)). The UV blocked region (dark), which forms the wall of hydrogel microwells, consists only of single-crosslinked networks produced by the aforementioned Schiff base reaction, whereas the UV exposed regions (red), which form the floors of hydrogel microwells, consist of dual-crosslinked networks produced by both the chemical crosslinking and photocrosslinking mechanisms.

To illustrate the versatility of this approach, dual-crosslinked micropatterned OMA/PEG hydrogel microwells with different microwell sizes were prepared. By using photomasks with grid patterns of different dimensions [500 (Fig. 2(a)) and 100 μm (Fig. 2(b))], hydrogel microwells with different well sizes that mirrored the photomasks were successfully generated. Wall heights of the hydrogel microwells formed with 500 μm pattern were significantly greater than those of the hydrogel microwells formed with 100 μm pattern (Fig. 2(d)). Interestingly, it was found that when the differential swelling of hydrogel microwells was induced in diH_2O, resulting wall heights were significantly greater than when DMEM or DPBS was used.

To show the potential utility of the OMA/PEG hydrogel microwells for controlled, sustained and localized delivery of

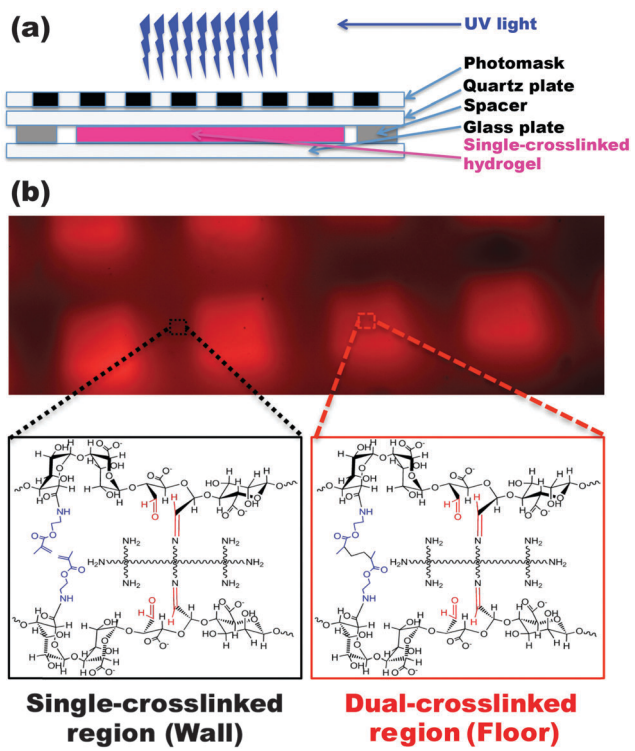

Fig. 1 Fabrication of a dual-crosslinked microwell hydrogel. (a) Schematic depicting the creation of a micropatterned dual-crosslinked OMA/PEG microwell hydrogel. (b) Fluorescence photomicrograph of a micropatterned dual-crosslinked OMA/PEG microwell hydrogel with a 100 μm grid pattern. The UV blocked region (dark) consists only of a single-crosslinked network formed by Schiff base reaction between the aldehyde groups of the OMA and the amine groups of the 8-arm PEG, whereas the UV exposed regions (red) consist of dual-crosslinked networks formed by both chemical crosslinking and photocrosslinking.

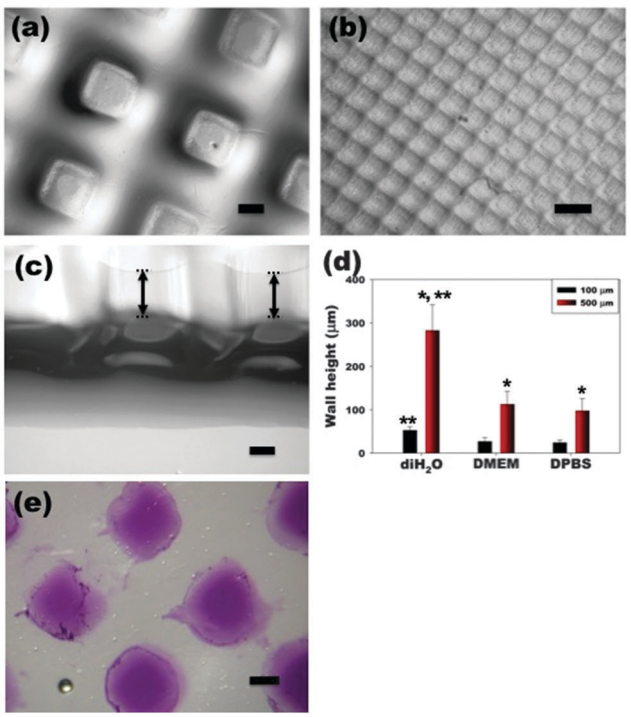

Fig. 2 Optical photomicrographs and wall height measurement of dual-crosslinked OMA/PEG microwell hydrogels with various pattern sizes. Dual-crosslinked OMA/PEG hydrogel microwells formed with (a) 500 μm and (b) 100 μm grid patterns. (c) A cross section of the dual-crosslinked OMA/PEG hydrogel microwells formed with the 500 μm grid pattern. (d) Wall height of dual-crosslinked OMA/PEG hydrogel microwells after differential swelling of the hydrogels was induced in diH_2O, DMEM or DPBS. *$p < 0.05$ compared to 100 μm. **$p < 0.05$ compared to DMEM and DPBS. (e) Immobilization of heparin on the bottom of the hydrogel microwell as demonstrated by toluidine blue O staining. The scale bars indicate 250 μm.

Table 1 Shear storage modulus of dual-crosslinked OMA/PEG hydrogels

	PEG		
	5% w/v	10% w/v	20% w/v
OMA (20%[a])	27 ± 3 kPa	35 ± 2 kPa*	37 ± 3 kPa*
	OMA		
	9%[a]	14%[a]	20%[a]
PEG (20% w/v)	65 ± 19 kPa	47 ± 16 kPa	37 ± 3 kPa**

[a] Actual oxidation of uronic acid units was calculated from ^{1}H-NMR data. *$p < 0.05$ compared to 5% w/v PEG. **$p < 0.05$ compared to 9% OMA.

bioactive molecules from the bottom of the well, heparin, which can bind to many growth factors through affinity interactions,[30,32] was micropatterned into the hydrogel. Toluidine blue o staining (purple color) demonstrates the presence of heparin covalently coupled only on the bottom of the hydrogel microwells (Fig. 2(e)). In the future, the covalently bound heparin may be used to control the delivery of heparin binding growth factors incorporated into the system during microwell fabrication or to sequester and then release these factors when they are present in the culture medium.

The shear storage moduli of unpatterned dual-crosslinked OMA/PEG hydrogels were measured to examine the effects of PEG concentration and the degree of alginate oxidation on the mechanical properties of hydrogel microwells formed by this dual-crosslinking strategy (Table 1). As the actual oxidation of the alginate increased from 9% to 20%, the average storage modulus decreased from 65 kPa to 37 kPa. This finding is supported by our previous study which showed that the storage modulus of photocrosslinked OMA hydrogels without 8-arm PEG-amine decreased as the oxidation level of the OMA increased.[28] Since increasing the concentration of 8-arm PEG-amine from 5 to 20% w/v increases the number of single-crosslinked networks formed in the dual-crosslinked hydrogels, the average storage modulus of the dual-crosslinked hydrogels increased from 27 kPa to 37 kPa. These results indicate that the stiffness of the dual-crosslinked hydrogels is easily controllable by varying the alginate oxidation level and polymer concentration, which may allow for tuning the mechanical properties of the microwells in this system.

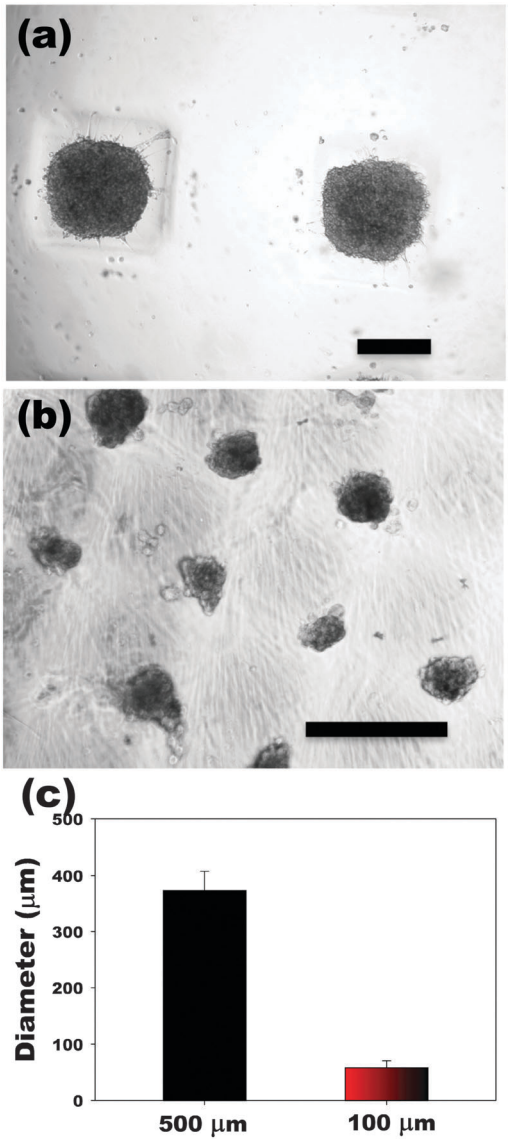

Fig. 3 Formation of hASCs spheroids. Optical photomicrographs of hASC spheroids in the dual-crosslinked OMA/PEG hydrogel microwells formed with (a) 500 μm and (b) 100 μm grid patterns. (c) Diameter of hASC multicellular spheroids formed in hydrogel microwells. The scale bars indicate 250 μm.

Formation of multicellular 3D hASC spheroids

While microwell techniques have demonstrated the ability to form multicellular spheroids,[20,22,23,40,41,43,46] to our best knowledge, there has not been a report of soluble cues such as growth factors and cytokines being delivered from a microwell platform used to form and culture cell spheroids. Here, we present a simple but robust approach for controlling multicellular spheroid sizes while simultaneously delivering bioactive molecules from the microwell culture substrate itself using micropatterned dual-crosslinked OMA/PEG hydrogel microwells. The use of dual-crosslinked OMA/PEG hydrogel microwells yielded relatively uniform hASC spheroids, which scaled in size with the dimensions of the micropatterned grid utilized. As shown in Fig. 3, the 500 μm grid-patterned hydrogel microwells resulted in larger hASC spheroids (mean diameter = 373 ± 34 μm, Fig. 3(a) and (c)) compared to 100 μm grid-patterned hydrogel microwells (mean diameter = 59 ± 12 μm, Fig. 3(b) and (c)). The viability of the cultured hASC spheroids was evaluated by a Live/Dead assay to examine cell survival during culture in the OMA/PEG hydrogel microwells. High cell viability was observed throughout the spheroids both at day 1 and 4 (Fig. 4) in microwells of both sizes, indicating that the whole system, including the process of spheroid formation, the OMA/PEG hydrogels themselves and degradation products, are cytocompatible. Since a simple yet robust method that provides precise control over multicellular spheroid size has

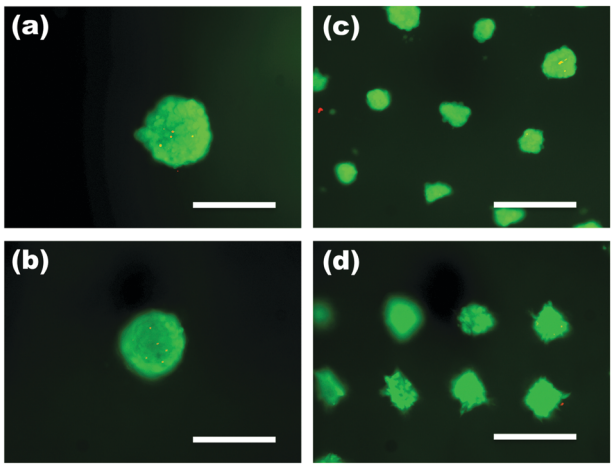

Fig. 4 Viability of hASC spheroids. Fluorescence photomicrographs of live (green) and dead (orange-red) cells in hASC spheroids in the dual crosslinked OMA/PEG microwell hydrogels formed with 500 μm grid patterns at (a) day 1 and (b) day 4 and with 100 μm grid patterns at (c) day 1 and (d) day 4. The scale bars indicate 200 μm.

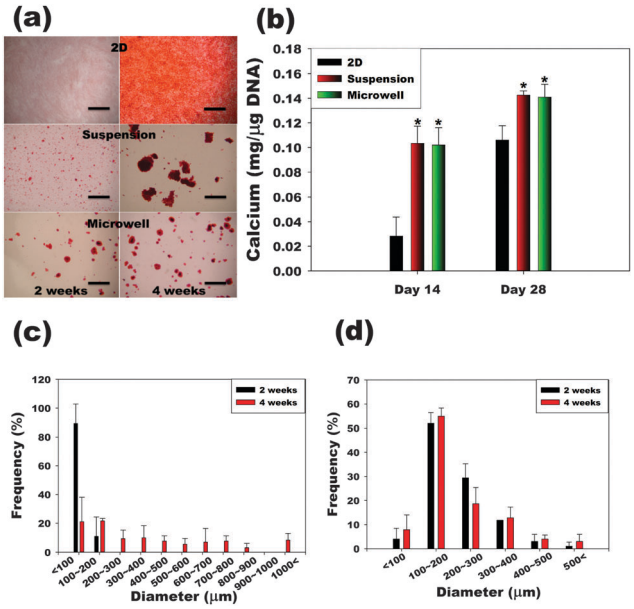

Fig. 5 Osteogenic differentiation of hASC. (a) Alizarin red S stained images of hASCs in traditional two-dimensional culture on tissue culture plastic (2D), conventional suspension culture in a spinner flask (Suspension), and suspension culture of spheroids in hydrogel microwells a spinner flask (Microwell). The scale bars indicate 2 mm. (b) Quantification of calcium content normalized to the DNA. *$p < 0.05$ compared to 2D at specific time point. Size distribution of hASC multicellular spheroids in the (c) Suspension and (d) Microwell groups.

not previously been demonstrated, the micropatterned dual-crosslinked OMA/PEG hydrogel microwell system developed in this study could be a useful platform to investigate the effect of multicellular spheroid size on the behavior of stem cells.

Osteogenic differentiation of multicellular 3D hASC spheroids

To demonstrate the feasibility of driving osteogenic differentiation of multicellular 3D hASC spheroids using this system, hASC spheroids were formed in BMP-2-laden dual-crosslinked OMA/PEG hydrogel microwells and cultured in a spinner flask containing osteogenic differentiation media without BMP-2. Since mineralization is the ultimate indicator of osteogenic differentiation of hASCs, it was evaluated by Alizarin red S staining and quantification of calcium content. As shown in Fig. 5(a) and (b), mineralization of hASCs increased from 2 to 4 weeks when cultured on standard tissue culture plastic (2D) in osteogenic media containing BMP-2. When a suspension of individual hASC were cultured in osteogenic differentiation media containing BMP-2 in a spinner flask (Suspension), their mineralization was significantly higher compared to standard 2D culture at both time points. When hASC spheroids formed in hydrogel microwells containing BMP-2 were cultured in a spinner flask containing osteogenic differentiation media without BMP-2 (Microwell), they also mineralized significantly more than the standard 2D culture at 2 and 4 weeks. Importantly, similar levels of mineralization were observed at both time points when less BMP-2 (total 12 μg for 4 weeks) was delivered from the hydrogel microwells (Microwell) compared to when BMP-2 (total 43.2 μg for 4 weeks) was delivered in the spinner flask media (Suspension). These results indicate that, for the experimental conditions examined, culture of individual hASCs and hASC spheroids in spinner flasks containing osteogenic media resulted in enhanced mineralization compared to 2D culture. Additionally, BMP-2 released from the hydrogel microwells was bioactive as it drove osteogenic differentiation of hASC spheroids to a similar degree to that achieved with BMP-2 present in the culture media. Since photocrosslinkable heparin can be easily coupled to the network structure of methacrylated alginate hydrogel systems,[30] such an approach could be applied to sustain the delivery of heparin-binding growth factors from the microwells to increase their therapeutic efficacy.

The size and homogeneity of multicellular spheroids formed in the hydrogel microwells (Microwell) was maintained for up to 4 weeks of spinner flask suspension culture (Fig. 5(d)), while the size and inhomogeneity of cell spheroids formed by individual cell coalescence in spinner flask culture (Suspension) increased (Fig. 5(c)). The mean diameter of the Microwell group spheroids was significantly larger than that of the Suspension group spheroids at an early time point. After 2 weeks of suspension culture, the spheroid diameter was 204.91 ± 88.94 μm in the Microwell group, whereas there were few spheroids with an average diameter of 47.74 ± 34.87 μm in the Suspension group. After 4 weeks of suspension culture, the spheroid diameters were 209.21 ± 107.33 and 305.98 ± 306.59 μm in the Microwell and the Suspension group, respectively. A potential problem in cell aggregate culture is that necrosis can occur in the core of larger aggregates because of diffusional limitation of nutrients and oxygen.[39] In the multicellular spheroid culture (Microwell), an average aggregate diameter of approximately 200 μm was maintained for the entire culture period. Decreased aggregate size may permit enhanced maintenance of cell viability *in vitro* culture for a variety of cell types.[24,47,48]

Conclusion

In this study, a novel biodegradable, cytocompatible alginate-PEG hydrogel microwell system, which could be used for multicellular spheroid formation, was fabricated by a micropatterning technique. By changing the micropattern size, the size of the hydrogel microwells was easily controllable. Microwell-seeded hASCs generated multicellular spheroids of relatively uniform size and high cell viability. hASC spheroids formed in this manner exhibited rapid mineralization in osteogenic media with BMP-2 presented from the microwell hydrogels. This mineralization was more extensive than that of conventional 2D cultured hASCs in the same amount of time. This new microwell system may have great potential for future studies requiring rapid and easy multicellular spheroid formation of controllable sizes. In the future, the alginate comprising the microwells may also be modified to locally regulate the hydrogel's biochemical and/or physical properties, such as its stiffness or cell adhesivity, which would allow for control over presentation of these signals to cultured spheroids.

Acknowledgements

The authors gratefully acknowledge funding from the National Institutes of Health's National Institute of Arthritis and Musculoskeletal and Skin Diseases under award numbers R01AR063194 (EA), R21AR061265 (EA), R01AR066193 (EA) and T32AR007505 (OJ), and the National Institute of Dental & Craniofacial Research under award number R56DE022376 (EA). The contents of this publication are solely the responsibility of the authors and do not necessarily represent the official views of the National Institutes of Health.

References

1 D. Baksh, R. Yao and R. S. Tuan, *Stem Cells*, 2007, **25**, 1384–1392.
2 O. Jeon and E. Alsberg, *Adv. Funct. Mater.*, 2013, **23**, 4765–4775.
3 M. F. Pittenger, A. M. Mackay, S. C. Beck, R. K. Jaiswal, R. Douglas, J. D. Mosca, M. A. Moorman, D. W. Simonetti, S. Craig and D. R. Marshak, *Science*, 1999, **284**, 143–147.
4 P. S. In 't Anker, S. A. Scherjon, C. Kleijburg-van der Keur, G. M. de Groot-Swings, F. H. Claas, W. E. Fibbe and H. H. Kanhai, *Stem Cells*, 2004, **22**, 1338–1345.
5 P. A. Zuk, M. Zhu, H. Mizuno, J. Huang, J. W. Futrell, A. J. Katz, P. Benhaim, H. P. Lorenz and M. H. Hedrick, *Tissue Eng.*, 2001, **7**, 211–228.
6 O. Jeon, D. S. Alt, S. W. Linderman and E. Alsberg, *Adv. Mater.*, 2013, **25**, 6366–6372.
7 S. Schreml, P. Babilas, S. Fruth, E. Orso, G. Schmitz, M. B. Mueller, M. Nerlich and L. Prantl, *Cytotherapy*, 2009, **11**, 947–957.
8 O. Jeon, J. W. Rhie, I. K. Kwon, J. H. Kim, B. S. Kim and S. H. Lee, *Tissue Eng., Part A*, 2008, **14**, 1285–1294.
9 F. Verseijden, H. Jahr, S. J. Posthumus-van Sluijs, T. L. Ten Hagen, S. E. Hovius, A. L. Seynhaeve, J. W. van Neck, G. J. van Osch and S. O. Hofer, *Tissue Eng., Part A*, 2009, **15**, 445–452.
10 H. J. Kim, S. H. Park, J. Durham, J. M. Gimble, D. L. Kaplan and J. L. Dragoo, *J. Tissue Eng.*, 2012, **3**, 2041731412466405.
11 F. H. Shen, B. C. Werner, H. Liang, H. Shang, N. Yang, X. Li, A. L. Shimer, G. Balian and A. J. Katz, *Spine J.*, 2013, **13**, 32–43.
12 P. C. Baer, N. Griesche, W. Luttmann, R. Schubert, A. Luttmann and H. Geiger, *Cytotherapy*, 2010, **12**, 96–106.
13 C. Brannmark, A. Paul, D. Ribeiro, B. Magnusson, G. Brolen, A. Enejder and A. Forslow, *PLoS One*, 2014, **9**, e113620.
14 H. F. Chan, Y. Zhang, Y. P. Ho, Y. L. Chiu, Y. Jung and K. W. Leong, *Sci. Rep.*, 2013, **3**, 3462.
15 S. H. Hsu, T. T. Ho, N. C. Huang, C. L. Yao, L. H. Peng and N. T. Dai, *Biomaterials*, 2014, **35**, 7295–7307.
16 S. H. Hsu and G. S. Huang, *Biomaterials*, 2013, **34**, 4725–4738.
17 N. C. Cheng, S. Y. Chen, J. R. Li and T. H. Young, *Stem Cells Transl. Med.*, 2013, **2**, 584–594.
18 L. L. Dunlop and B. K. Hall, *Int. J. Dev. Biol.*, 1995, **39**, 357–371.
19 S. Egawa, S. Miura, H. Yokoyama, T. Endo and K. Tamura, *Dev., Growth Differ.*, 2014, **56**, 410–424.
20 G. Pettinato, X. Wen and N. Zhang, *Sci. Rep.*, 2014, **4**, 7402.
21 M. Cordey, M. Limacher, S. Kobel, V. Taylor and M. P. Lutolf, *Stem Cells*, 2008, **26**, 2586–2594.
22 A. B. Bernard, C. C. Lin and K. S. Anseth, *Tissue Eng., Part C*, 2012, **18**, 583–592.
23 S. E. Yeon, Y. No da, S. H. Lee, S. W. Nam, I. H. Oh, J. Lee and H. J. Kuh, *PLoS One*, 2013, **8**, e73345.
24 T. J. Bartosh, J. H. Ylostalo, A. Mohammadipoor, N. Bazhanov, K. Coble, K. Claypool, R. H. Lee, H. Choi and D. J. Prockop, *Proc. Natl. Acad. Sci. U. S. A.*, 2010, **107**, 13724–13729.
25 J. M. Kelm, N. E. Timmins, C. J. Brown, M. Fussenegger and L. K. Nielsen, *Biotechnol. Bioeng.*, 2003, **83**, 173–180.
26 M. Navarro and J. A. Planell, *Nanotechnology in regenerative medicine: methods and protocols*, Humana Press, Springer, New York, 2011.
27 O. Jeon, J. E. Samorezov and E. Alsberg, *Acta Biomater.*, 2014, **10**, 47–55.
28 O. Jeon, D. S. Alt, S. M. Ahmed and E. Alsberg, *Biomaterials*, 2012, **33**, 3503–3514.
29 B. Neu, J. K. Armstrong, T. C. Fisher and H. J. Meiselman, *Biorheology*, 2003, **40**, 477–487.
30 O. Jeon, C. Powell, L. D. Solorio, M. D. Krebs and E. Alsberg, *J. Controlled Release*, 2011, **154**, 258–266.
31 L. L. Gosey, R. M. Howard, F. G. Witebsky, F. P. Ognibene, T. C. Wu, V. J. Gill and J. D. MacLowry, *J. Clin. Microbiol.*, 1985, **22**, 803–807.
32 S. S. Shah, M. Kim, K. Cahill-Thompson, G. Tae and A. Revzin, *Soft Matter*, 2011, **7**, 3133–3140.
33 B. T. Estes, B. O. Diekman, J. M. Gimble and F. Guilak, *Nat. Protoc.*, 2010, **5**, 1294–1311.

34 Q. Z. Zhang, A. L. Nguyen, S. H. Shi, C. Hill, P. Wilder-Smith, T. B. Krasieva and A. D. Le, *Stem Cells Dev.*, 2012, **21**, 937–947.
35 W. J. Wang, K. Itaka, S. Ohba, N. Nishiyama, U. I. Chung, Y. Yamasaki and K. Kataoka, *Biomaterials*, 2009, **30**, 2705–2715.
36 Q. H. Zhang, X. G. Chen, G. H. Cui and W. W. Zheng, *DNA Cell Biol.*, 2007, **26**, 497–503.
37 N. S. Hwang, S. Varghese and J. Elisseeff, *Adv. Drug Delivery Rev.*, 2008, **60**, 199–214.
38 E. J. Lee, S. J. Park, S. K. Kang, G. H. Kim, H. J. Kang, S. W. Lee, H. B. Jeon and H. S. Kim, *Mol. Ther.*, 2012, **20**, 1424–1433.
39 G. Mehta, A. Y. Hsiao, M. Ingram, G. D. Luker and S. Takayama, *J. Controlled Release*, 2012, **164**, 192–204.
40 Y. Y. Choi, B. G. Chung, D. H. Lee, A. Khademhosseini, J. H. Kim and S. H. Lee, *Biomaterials*, 2010, **31**, 4296–4303.
41 G. S. Jeong, J. H. Song, A. R. Kang, Y. Jun, J. H. Kim, J. Y. Chang and S. H. Lee, *Adv. Healthcare Mater.*, 2013, **2**, 119–125.
42 J. Fukuda and K. Nakazawa, *Tissue Eng.*, 2005, **11**, 1254–1262.
43 Y. S. Hwang, B. G. Chung, D. Ortmann, N. Hattori, H. C. Moeller and A. Khademhosseini, *Proc. Natl. Acad. Sci. U. S. A.*, 2009, **106**, 16978–16983.
44 E. Alsberg, H. A. von Recum and M. J. Mahoney, *Expert Opin. Biol. Ther.*, 2006, **6**, 847–866.
45 O. Jeon and E. Alsberg, *Tissue Eng., Part A*, 2013, **19**, 1424–1432.
46 C. L. Bauwens and M. D. Ungrin, *Methods Mol. Biol.*, 2014, **1181**, 15–25.
47 E. Curcio, S. Salerno, G. Barbieri, L. De Bartolo, E. Drioli and A. Bader, *Biomaterials*, 2007, **28**, 5487–5497.
48 Z. Wen, Q. Liao, Y. Hu, L. You, L. Zhou and Y. Zhao, *Braz. J. Med. Biol. Res.*, 2013, **46**, 634–642.